*remote sensing*

MDPI

*Article*

# Compact Mesoscale Eddies in the South Brazil Bight

**Cesar B. Rocha [1,*] and Iury T. Simoes-Sousa [2]**

[1] Department of Marine Sciences, University of Connecticut, Groton, CT 06340, USA
[2] College of Engineering, University of Massachusetts Dartmouth, Dartmouth, MA 02747, USA
* Correspondence: cesar.rocha@uconn.edu

**Abstract:** Recent studies suggest that the South Brazil Bight (SBB) hosts strong westward propagating mesoscale eddies. We use 28 years of satellite altimetry data and a new Eddy Atlas to estimate how much of the eddy kinetic energy (EKE) observed in the SBB is accounted for by local eddies, generated in the Brazil Current (BC) region, versus remote eddies generated eastward of the BC region. First, we estimate a BC frontal density to obtain a robust definition of BC region. The BC front is well-defined throughout the SBB, occupying the region between the 200-m and 1000-m isobath, except in eddy hotspots downstream of sharp inflections of the continental slope, where the EKE far exceeds the mean kinetic energy (MKE). Compact, closed-contour mesoscale eddies account for 30–50% of the total EKE observed in the SBB, with local eddies accounting for most of the compact EKE in the BC region, defined as the area within 200 km of the 28-year mean BC front. Remote compact eddies account for less than 10% of the EKE observed in the BC region; compact eddies generated at long distances from the SBB, including eddies generated in the Southeastern Atlantic, contribute an insignificant fraction of EKE in the BC region.

**Keywords:** Brazil Current; mesoscale eddies; South Brazil Bight



**Citation:** Rocha, C.B.; Simoes-Sousa, I.T. Compact Mesoscale Eddies in the South Brazil Bight. *Remote Sens.* **2022**, *14*, 5781. https://doi.org/10.3390/rs14225781

Academic Editor: Vladimir N. Kudryavtsev

Received: 13 September 2022
Accepted: 12 November 2022
Published: 16 November 2022



## 1. Introduction

Beginning with Topex/Poseidon (TP), modern nadir-looking high-accuracy satellite altimetry has revolutionized oceanography [1]. Since 1992, the TP/Jason and European Remote-Sensing (ERS) series have provided a reliable window into ocean processes hitherto essentially inaccessible to oceanographers. Satellite altimetry revealed that about 80–90% of the ocean kinetic energy is accounted for by mesoscale variability due to linear Rosbby waves and nonlinear waves and eddies, with lateral scales of tens to hundreds of kilometers and timescales longer than a few days [2]. Key to this finding is that at these scales ocean flows are in geostrophic balance, implying that sea surface height (SSH) is a streamline of the flow. With a constellation of satellite altimeters, the ocean surface topography is now routinely mapped on a daily to weekly basis, providing a mesoscale context to localized oceanographic experiments and constraining general circulation models, among many other applications.

Using ten years of sea-level anomalies collected by TP and ERS-1/2, Chelton et al. [3,4] showed that nonlinear mesoscale eddies account for most of the sea-surface variability previously attributed to Rosbby waves [5,6] (Challenges to this interpretation do exist: see Oliveira and Polito [7] and Polito and Sato [8]). Chelton et al.'s finding is a confirmation of anecdotal evidence arising from the pioneering Mid-Ocean Dynamcis Experiment [9] as well as theoretical and numerical models that hinted on vigorous nonlinear mesoscale variability even away from strong western boundaries (e.g., [10]). Indeed, mesoscale eddies are critical to the equilibration of the large-scale ocean circulation and contribute most of the lateral stirring and mixing of ocean biogeochemical tracers and other climate-relevant ocean properties (e.g., [11–13]). Characterizing mesoscale eddying processes and their impacts on ocean physics and biogeochemistry is critical to better understanding and modeling the ocean's role in climate variability and change.

The work by Chelton et al. (2007, 2011) began such characterization on a global scale. Further, since the late aughts, several regional studies appeared, focusing on regions and aspects of mesoscale eddies (e.g., [14–18]); however, mesoscale eddies remain poorly studied in many places of the world ocean. One of such places is the Brazil Current region in the Southwestern Atlantic. Eddy kinetic energy maps of the South Atlantic have two bright spots (Figure 1). One is the Agulhas Retroflection region, off the southern tip of Africa, where the Agulhas Current runs out of the continental grip and violently veers eastwards, shedding Agulhas Rings in the process [19]. These rings are some of the largest mesoscale anticyclones in the world ocean, and drift northwest into the South Atlantic (e.g., [20]). The other bright spot is the Brazil-Malvinas Confluence, off Argentina, where the southward flowing Brazil Current collides head-on with the northward flowing Malvinas/Falkland Current, developing vigorous mesoscale variability as they separate from the boundary [21,22]. Mesoscale studies in the South Atlantic have almost exclusively focused on these two regions.

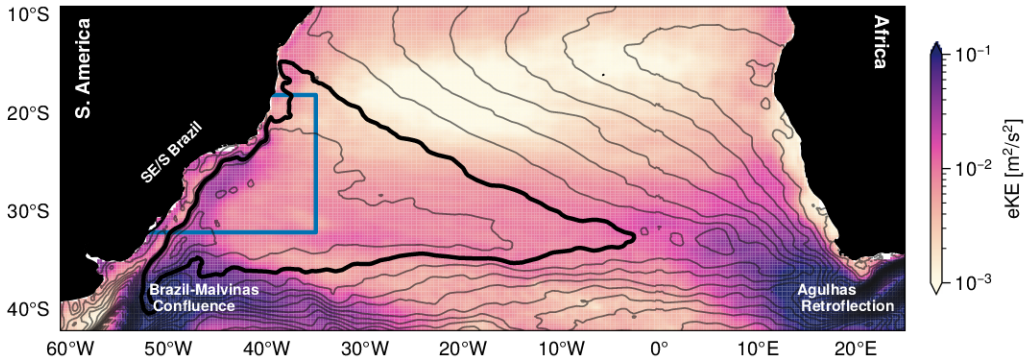


**Figure 1.** The surface circulation and variability of the subtropical South Atlantic as depicted by the CNES-CLS18 mean dynamic topography (MDT) contoured every 0.05 m (black lines) and the surface eddy kinetic energy from 28 years of satellite altimetry (colors). The thick black line is the longest closed contour of MDT = 0.60 m, one of the outermost closed contours of the South Atlantic Subtropical Gyre and a good proxy for the time-mean Brazil Current front off Southeast and South Brazil. The blue lines define the regional focus area of this study.

Much less studied is the region between 20°S and 32°S in the Southwestern Atlantic—a secondary maximum in eddy kinetic energy (Figure 1). Analyses of mooring velocity time series and and linear instability models show that mesoscale variability in this region is driven by local baroclinic instability, which leads to Brazil Current meandering and eddy shedding (e.g., [23,24]); however, a number of recent studies suggest that remotely generated, westward propagating eddies are also observed in the region [25–29].

Guerra et al. [25] and Laxenaire et al. [26,27] contend that some of these remote eddies are remnant Agulhas Rings, whose transatlantic journeys can be followed with automated eddy tracking algorithms applied to gridded sea-level anomaly maps. While these Rings have been recognized for long as a conduit of warm, salty Indian waters into the South Atlantic [19], evidence that they collide with the BC has eluded oceanographers for nearly two decades: most Agulhas Rings disappear or severely weaken in the altimetric record as they negotiate the Walvis Ridge in the Southeastern Atlantic. With a hybrid tracking algorithm, Guerra et al. [25] were able to identify over 120 Rings whose surface expression survived the crossing of the Ridge. Using another tracking algorithm, one that allows for eddy splitting and merging, Laxenaire et al. [26] identified over one hundred Rings, many of which seem to make their way to the Brazilian coast. Guerra et al. [25] presents observational evidence of one such decaying Agulhas Ring colliding with the Brazil Current, after a 3.5-year journey of 3500 km. A mooring off Cabo Frio (22°S) observed the Ring, whose vertical structure was largely baroclinic and intensified at 200–300 m. This contrasts

with more barotropic and surface-intensified Brazil Current eddies observed at the mooring before and after this event.

Napolitano et al. [28] also showed evidence of the arrival of remote eddies at the western boundary. The authors used observations and a regional simulation nested from a South Atlantic simulation to study the dynamics of the Brazil Current and its undercurrent, the Intermediate Western Boundary Current, at 21°S. Napolitano et al.'s model revealed the consistent arrival of remote eddies, both cyclones and anticyclones, drifting westward at approximately the phase speed of non-dispersive baroclinic Rosbby waves. Napolitano et al. [28] remark that these remote eddies strongly interact with the boundary currents, "experiencing explosive downstream growth through horizontal shear production". Similar to the eddy reported by Guerra et al. [25], the remote eddies in Napolitano et al.'s model were intensified at 300–400 m, different from the vertical structure of local Brazil Current eddies.

Building on the studies of Laxenaire et al. [26] and Laxenaire et al. [27]—accounting for vortex merging and splitting—Ioannou et al. [29] argue that many of the remote eddies that arrive in the Southwestern Atlantic basin can be tracked back to the Benguela Current upwelling region. Of the westward propagating eddies in Ioannou et al. [29] that propagate across the South Atlantic, eventually arriving in the SBB, many undergoe several events of merging and splitting. (It is unclear whether fluid from the Benguela Current upwelling region remains trapped after merging and splitting.)

While these recent studies present evidence that some remote eddies—remnant Agulhas Rings and other eddies—may arrive at the Brazil Current region, a quantification of how much these eddies contribute to the local eddy kinetic energy (c.f., Figure 1) is missing. The goal of this paper is to make such quantification, obtaining a statistical description of the mesoscale eddy variability in the Brazilian continental margin upstream of the Brazil-Malvinas Confluence and its partition into local and remote contributions. Our regional focus is centered in the South Brazil Bight (SBB). Although technically the SBB extends only from Cabo Frio (23°S) to Cabo Santa Marta Grande (28.5°S), we herein refer to SBB loosely as the blue regional box in Figure 1, which extends to 32°S. A main motivation for studying the partition of mesoscale eddies in the SBB into local versus remote eddies is to characterize the origin of the variability of the Brazil Current and its transport of volume, heat and other climate-relevant tracers. The statistical partitioning presented here also provides a benchmark to test the skill of numerical models in simulating the circulation of the Southwestern Atlantic.

We use the term mesoscale eddies to refer to long-lived compact mesoscale structures. By compact we mean localized perturbations that are identified as extrema in high-pass maps of sea-surface height (c.f., [4]). Most eddies tracked in the original study of Chelton et al. [4] and in the Mesoscale Eddy Atlas used here [30] are nonlinear for they have particle velocities much larger than their propagation speeds, and thus possibly trap fluid for weeks to months; however, these eddies may not be formally coherent by other metrics (e.g., [31]) and, for this reason, we avoid referring to them as "coherent eddies" or "Lagrangian coherent structures." Our conservative wording, however, should not downplay the relevance of these eddies for the circulation, dynamics and biogeochemistry of the Southwestern Atlantic.

## 2. Material and Methods

### *2.1. Datasets*

#### 2.1.1. Gridded Sea-Level Product and Mean Dynamic Topography

To look at variability of the Brazil Current front and to estimate the kinetic energy due to compact mesoscale eddies, we use level-4 data of daily global sea-level and derived fields produced by the Segment Sol Multimission Altimetry and Orbitography of the Data Unification Altimeter Combination System (SSALTO/DUACS) and distributed by the Copernicus Marine Environment Monitoring Service Marine Services (CMEMS). Specifically, we use the delayed-time (reprocessed) all-satellite data product, spanning

28 years from January 1993 through December 2021. This product provides both sea-level anomaly (SLA), absolute dynamic topography (ADT), derived geostrophic velocities (from both SLA and ADT), and formal errors from statistical mapping of level-3 (along-track) data onto a $1/4^\circ \times 1/4^\circ$ grid. For reference, the CMEMS identification for this product is SEALEVEL_GLO_PHY_CLIMATE_L4_MY_008_057. Previous versions of this product were referred to in the oceanographic literature as "AVISO product," because they were distributed by the French Space Agency's AVISO service (Archiving, Validation and Interpretation of Satellite Oceanographic). Herein we refer to it as CMEMS sea-level product.

In addition to the CMEMS sea-level product, we use the CNES-CLS18 mean dynamic topography (MDT), a 1993–2017 time-mean, $1/8^\circ$ global sea surface derived from a combination of altimetric and gravimetric satellite data, surface wind reanalysis, and in-situ drifter and hydrographic observations. Mulet et al. [32] describes the details of the CNES-CLS18 MDT solution and compares it against its predecessor (CNES-CLS13). The CNES-CLS18 MDT is distributed by Aviso+ (https://www.aviso.altimetry.fr; last access: 5 April 2022).

#### 2.1.2. Eddy Atlas

A central component of this study is the characterization of the mesoscale eddy kinetic energy due to compact mesoscale eddies identified in sea-level maps. For this purpose, we employ the Mesoscale Eddy Trajectory Atlas META3.2 DT, a new eddy tracking census that supersedes previous products distributed by AVISO or CMEMS. Specifically we use the delayed-time all-satellite atlas (META3.2 DT DT all-satellites, DOI : 10.24400/527896/a01-2022.005.210802), which identifies eddies in the CMEMS product described above. Herein we refer to the META3.2 DT product as Eddy Atlas.

Pegliasco et al. [30] describes a beta version META3.2 DT Eddy Atlas, the META3.1exp product, and compares it against META2.0 and other atlases [4,33]. Only a few minor changes were made from the experimental version 3.1 to the current version 3.2 DT, and the description of 3.1exp in Pegliasco et al. [30] is overall valid for 3.2. A main novelty in META3.2 DT compared to META 2.0 is the identification of compact mesoscale eddies as closed contours of spatially high-pass filtered ADT in lieu of closed contours of filtered SLA. Use of ADT allows for better detection of eddies near strong currents and steep topography, and is key to a good representation eddies that grow locally on top of standing meanders. META3.2 DT also changed the eddy detection from the Chelton et al.'s eddy-tracking lineage of algorithms to an upgraded version of the algorithm by Mason et al. [33]. META3.2 DT further implemented a few minor changes to error thresholds, filtering of large-scale signals (reducing the half-power scale from 1000 km to 700 km), a reduced sea-level interval to search for the eddy edges, etc. Globally, META3.2 DT has an increased number of eddies compared to META2.0, but most of these extra eddies are small, short-lived eddies and will not be considered in our analysis. We also discard eddies whose time-mean amplitudes are smaller than 2.5 cm, whose lifetime is shorter than 4 weeks, and whose first detection are centered at depths shallower than 200 m, to avoid variability related to sampling noise and defective tidal corrections on the shelf.

In addition to basic eddy characteristics (trajectories, amplitude, swirl speed), META3.2 DT provides particulars for each eddy observation, including the coordinates for sea-level contours [30]. (A difference between 3.1 exp and 3.2 DT is that 20-point contours instead of 50-point contours are now provided.) These added details about the eddy shape allow us to estimate the kinetic energy accounted for by compact mesoscale eddies in the SBB. For reference, it is useful to define a few eddy properties that are frequently referred to in the text (updated from [30]):

- Effective contour: outermost high-pass filtered ADT closed contour detected from a search starting at the localized sea-level extremum; provided as 20-point coordinates (longitude, latitude).
- Speed contour: high-pass filtered ADT closed contour associated with maximum azimuthally averaged velocity detected from a search starting the localized sea-level extremum.

- Effective radius: eddy radius obtained by fitting a circle to the effective contour.
- Speed radius: eddy radius obtained by fitting a circle to the speed contour.
- Eddy center: coordinates (longitude, latitude) of the high-pass filtered ADT extremum obtained from fitting a circle to the speed contour.
- Average speed: azimuthally averaged speed associated with the speed radius.

### *2.2. The Brazil Current Front*

To partition the compact mesoscale eddy variability in the Brazil Current region into local and remote contributions, we first need a definition of local variability. To develop such definition, we investigate the position of the Brazil Current front in the SBB. Figure 1 depicts the 0.6-m contour of mean dynamic topography, one of the outermost closed contours of the South Atlantic Subtropical Gyre (c.f., [34]). One may be tempted to define the Brazil Current front as the 0.6-m contour of a time-averaged absolute dynamic topography, the sum of the mean dynamic topography and sea-level anomaly,

$$\langle \mathrm{ADT} \rangle = \mathrm{MDT} + \langle \mathrm{SLA} \rangle \,, \tag{1}$$

where angle brackets in (1) represent time average (e.g., monthly or yearly average), and `MDT` is the CNES-CLS18 mean dynamic topography solution described in Section 2.1. This definition needs careful consideration to account for a steric sea-level trend and large-scale sea-level variabilities unrelated to variations of the Brazil Current position. For simplicity, we start by analyzing yearly averaged fronts, then move to monthly averaged fronts.

#### 2.2.1. Yearly Averaged Front

A close inspection of yearly averaged ADT in the CMEMS sea-level product shows that the $\langle \mathrm{ADT} \rangle_{yr} = 0.6$-m contour slightly moved onshore with time over the 28-year satellite altimetry record; however, this shift is due to steric changes in sea level. As expected, an analysis of multi-year averaged maps of vertical vorticity, computed from averaged ADT, reveals no shift in the position of the Brazil Current jet (the line of zero vorticity between positive and negative voriticty flanks), suggesting no significant trends in the position of the Brazil Current front on the slope. This is consistent with the findings of Drouin et al. [34], who report no significant changes in the area of the South Atlantic Subtropical Gyre, despite the southward migration of the Gyre in response to intensifying westerly winds. Hence, to properly define the position of the Brazil Current front using ADT, we first need to account for this trend largely associated with ocean warming, whose changes in sea level do not alter the ocean circulation. We thus define the yearly averaged Brazil Current front as the 0.6-m contour of *detrended* absolute dynamic topography $\langle h \rangle_{yr}$,

$$\langle h \rangle_{yr} \stackrel{\text{def}}{=} \langle \mathrm{ADT} \rangle_{yr} - \mathrm{trend}\big(\langle \mathrm{ADT} \rangle_{yr}\big) \,, \tag{2}$$

where the linear trend is calculated via least-squares fitting of a straight line to the 28-year time series of `ADT` at every location. The Brazil Current front is not a unique contour $\langle h \rangle_{yr} = 0.6$ m: background circulation and errors in tidal correction on the shelf as well as residual eddy variability offshore sometimes imprint on the chosen contour; however, the Brazil Current front can be selected by finding the longest contour in the SBB and discarding closed contours.

#### 2.2.2. Monthly Averaged Front

While the $\langle h \rangle_{yr} = 0.6$-m contour defined above is a robust proxy for the yearly averaged Brazil Current position, the identification of the Brazil Current front is more challenging for shorter-term averages, such as monthly averages $\langle h \rangle_{mo}$ defined in analogy to yearly average ADT in (2). This is because large-scale intra-annual variability strongly modifies the regional $\langle h \rangle_{mo} = 0.6$-m contour, and selection of the longest contour fails to identify the Brazil Current front at least half of the time. (The signal of strong mesoscale

eddies are not an issue as they can be removed by disregarding closed contours.) Removing a regional mean every month takes care of most large-scale intra-annual variability, significantly improving the skill of the monthly Brazil Current front identification. We thus introduce a regional anomaly of the monthly averaged ADT:

$$h' \stackrel{\text{def}}{=} \langle h \rangle_{mo} - \overline{\langle h \rangle}_{mo}\,, \tag{3}$$

where overbar denotes space average over the region enclosed by the blue box in Figure 1. We define the Brazil Current front as longest $h' = 0.05$-m contour.

### 2.3. Mean and Eddy Kinetic Energy

We also compute the mean and eddy kinetic energies in the SBB. The mean kinetic energy is the kinetic energy of the long-term time-mean surface geostrophic flow associated with the mean dynamic topography:

$$\text{MKE} = \tfrac{1}{2}\left(\tfrac{g}{f}\right)^2 \left[(\partial_x \text{MDT})^2 + (\partial_y \text{MDT})^2\right], \tag{4}$$

where $g$ is the acceleration due to gravity and $f$ is the Coriolis parameter. The eddy kinetic energy is the kinetic energy of the geostrophic flow associated with the sea-level anomaly:

$$\text{EKE} = \tfrac{1}{2}\langle u^2 + v^2 \rangle\,, \tag{5}$$

where $(u, v)$ are the components of geostrophic velocity anomaly, calculated from the sea-level anomaly (SLA $=$ ADT $-$ MDT) and available as part of the CMEMS sea-level product. In addition, in (5), angle brackets denote time average over the entire record (28 years). (As standard in the oceanographic literature, we report the surface kinetic energy as energy per unit mass; kinetic energy per unit volume is obtained via multiplication of MKE and EKE by a reference density.) We emphasize that EKE defined above is the eddy kinetic energy of the surface geostrophic flow associated with all variability—not only due to compact mesoscale eddies—resolved in the CMEMS sea-level product.

### 2.4. Kinetic Energy of Mesoscale Eddies

To estimate the fraction of energy accounted for by compact mesoscale eddies, which are largely nonlinear and have the potential to trap water in their cores, we use the META3.2 DT Eddy Atlas. As described in Section 2.1, a main novelty of this atlas is that it provides, for each eddy observation, two contours identified by the automated eddy-tracking algorithm: the effective contour (outermost closed contour) and the speed contour (closed contour associated with maximum azimuthally averaged swirl speed).

To calculate the kinetic energy associated with the $i$th observation of a compact eddy $j$, we compute the arithmetic mean of the the geostrophic velocity anomalies squared from the sea-level product:

$$\texttt{EKE}_c(j, t_i) = \frac{1}{M}\sum_{i=k}^{M} \tfrac{1}{2}(u_k^2 + v_k^2)\,, \tag{6}$$

where the summation is carried over the points $k$ *inside* the effective contour at time $t = t_i$; $(u, v)$ are the geostrophic velocity anomalies in the sea-level product at time $t = t_i$. The estimate in (6) is similar to the definition of Chelton et al. [4], who calculated the kinetic energy of mesoscale eddies of compact form in a given coordinate $(x, y)$ by applying a time-dependent Kronecker-delta function to the velocity anomalies to select the points inside the contour, then averaging over time. Our estimate is time-dependent, and at each time $t_i$ the eddy is centered at a coordinate $(x_j, y_j)$. In other words, we have an estimate of the kinetic energy of each compact eddy during its lifetime, and we can use this estimate to calculate the total eddy kinetic energy due to compact eddies at a given location. Specifically, we calculate the arithmetic mean of $\texttt{EKE}_c(t_i, j)$ for all eddy observations (accounting for different eddies $j$ and different times $t_i$) in $0.25^\circ \times 0.25^\circ$ bins centered at the coordinates

of the CMEMS SLA product. The total eddy kinetic energy due to these eddies is referred to as $\mathtt{EKE}_c$, where the subscript $c$ stands for compact eddies. $\mathtt{EKE}_c$ is likely a lower-bound estimate to the contribution of compact mesoscale eddies to the total eddy kinetic energy in a given bin, because the effective contour is unlikely to contain all the sea-level variability of a given eddy (c.f., [4]). A similar estimate using the speed contour provides an even lower bound, and in the case of the SBB, the speed-contour estimate accounts for 20–30% less kinetic energy than the effective-contour estimate.

## 3. Results

### *3.1. Brazil Current Front*

Figure 2a shows a spaghetti diagram depicting $\langle h \rangle_{yr} = 0.6$-m contour for the 28-year altimetric record. Our $\langle h \rangle_{yr} = 0.6$-m method has high skill in identifying the yearly averaged Brazil Current front, which is well-defined in the SBB. By and large, the 28 contours are packed in the mid to upper slope, between the 200-m and 2000-m isobaths, showing the mean Brazil Current flowing largely along sinuous isobaths. One relevant exception is the region downstream of Cabo Frio at 23°S–25°S, where the yearly averaged Brazil Current front experiences large excursions about a longer-term mean MDT front, represented by the dashed orange line.

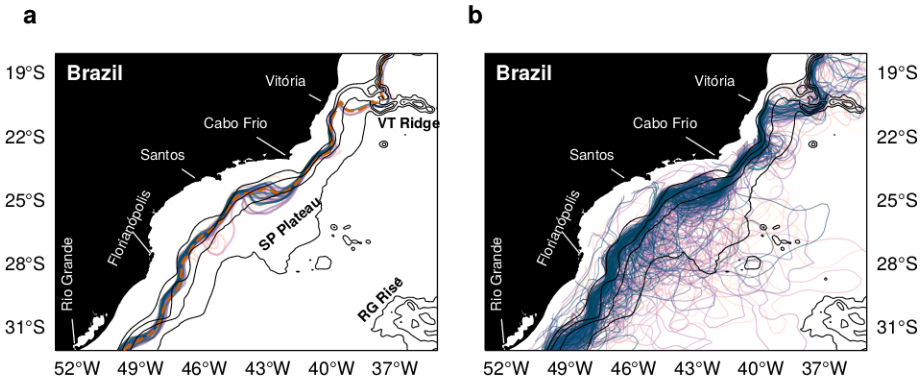


**Figure 2.** The Brazil Current front off Southeast and South Brazil as characterized by 28 years of satellite altimetry. (**a**) Yearly averaged fronts defined by 0.6-m contour of linearly detrended absolute dynamic topography ($h = 0.6$ m); the orange dashed line is the long-term mean front (MDT = 0.6 m). (**b**) Monthly averaged fronts defined by $h' = 0.05$ m, where $h'$ is monthly averaged $h$ (linearly detrended ADT) subtracted from a regional mean. The colors represent time, ranging from begining to end of the altimetric record. The land annotations are coastal cities in Brazil, used for geographical reference in the text. Key topographic features are also marked: Vitória-Trindade (VT) Ridge, São Paulo (SP) Plateau, and Rio Grande (RG) Rise. Solid black lines depict the 200, 1000, 2000 and 3000-m isobaths.

Figure 2b shows an angel-hair diagram depicting 1450 contours of $h' = 0.05$ m. As expected, the monthly averaged front shows much more variability than the yearly average front. Nonetheless, our single-contour method identifies the Brazil Current front flowing along the slope 90% of the time. Several contours do not connect the northern and southern edges of the SBB. They seem to separate from the slope on the southern edge of the São Paulo Plateau. As in the yearly averaged fronts case, there is significant spread in the frontal position downstream of Cabo Frio. The region south of Florianópolis and north of Rio Grande also displays strong frontal spread.

The contour maze in Figure 2b can be synthesized into a map of frontal density (c.f., [35]). We define the Brazil Current frontal density as the probability of finding—over the 28-year altimetric record—the $h' = 0.05$-m contour in 0.25° by 0.25° bins. The frontal density map in Figure 3a is a statistical characterization of the position of the Brazil Current front in the SBB. Pixels with high frontal density denote regions where the Brazil Current front is well defined and present for a large fraction of time. In other words, it is a pixel

where there is a high probability of finding the front in (frontal density equal to 1 means that the front is always found in the pixel). The opposite is true for pixels with low frontral density. To our knowledge, no such robust characterization has been previously reported throughout Southeast and South Brazil, including the SBB. Previous characterizations of the Brazil Current front in the region have focused on limited sea-surface temperature (SST) imagery [36] or more extensive analysis of SST images on smaller sub-regions of the SBB [35].

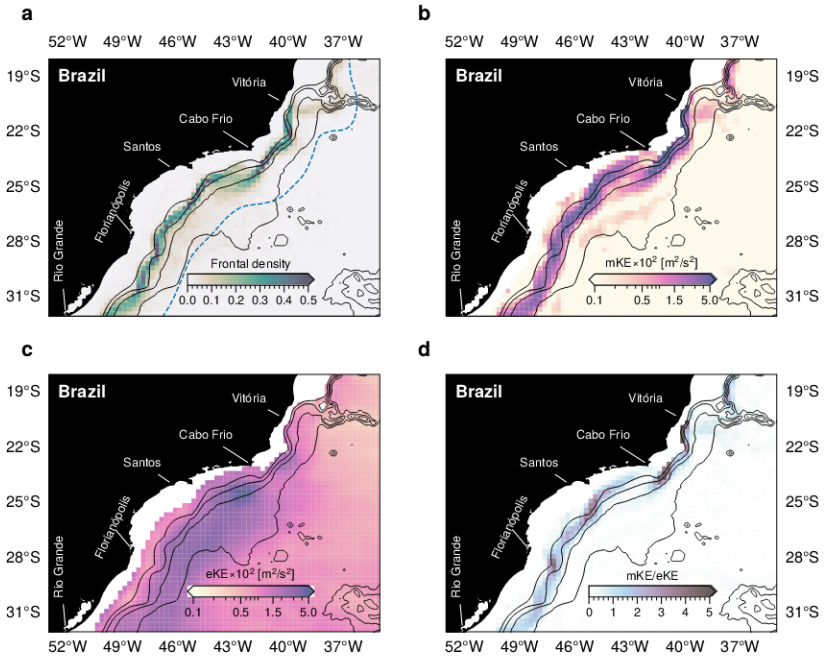


**Figure 3.** (**a**) Brazil Current frontal density defined by the probability of finding the monthly mean contour $h' = 0.05$ m in each $0.25° \times 0.25°$ pixel. (**b**) Mean surface kinetic energy (MKE) from the 28-year mean ADT. (**c**) Surface eddy kinetic energy (EKE) from 28 years of sea-level anomalies. (**d**) Ratio between mean and eddy kinetic energy, highlighting regions where the mean Brazil Current is stronger than its variability (dark purple) and regions dominated by mesoscale variability (white). The dashed blue line in (**a**) is the Brazil Current MDT front shifted 200-km due east; the Brazil Current region is defined as the area west of this curve. Solid black lines in (**a**,**c**) depict the 200, 1000, 2000 and 3000-m isobaths.

Figure 3b,c shows the kinetic energy of the long-term mean flow (MKE), the eddy kinetic energy (EKE), and their ratio (MKE/EKE). Consistent with the frontal density map, MKE is concentrated on the slope, with values as large as 0.06 $m^2\ s^{-2}$. The mean flow is significantly weaker in areas where the frontal density spreads out, such as the region downstream of Cabo Frio, where MKE is as low as 0.002 $m^2\ s^{-2}$. An offshore band of low MKE exists on the São Paulo Plateau, which may be related to a weak eddy-driven recirculation cell. The eddy component has a background kinetic energy level of 0.01 $m^2\ s^{-2}$ throughout the region and is significantly enhanced on the slope and adjacent areas over the São Paulo Plateau (Figure 3c). The region downstream of Cabo Frio presents a local maximum EKE, with values reaching 0.08 $m^2\ s^{-2}$, larger than the local MKE. The ratio MKE/EKE reveals that in several regions of the slope, especially at or downstream of changes in topographic orientation, EKE is at least as large as MKE, if not much larger. Downstream of Cabo Frio there is a 10,000 $km^2$ expanse where $\mathrm{MKE/EKE} \ll 1$. Lorenzzetti et al. [35] previously noted that the Brazil Current thermal front presents large variability in this region, and Rocha et al. [24] showed that 14-month velocity record from a mooring was barely enough to define a statistically significant mean flow at 24°S. The analysis of 28 years of altimetry confirms that this region is an eddy hotspot. It further suggests that other eddy hotspots exist, south of Florianópolis, all associated with dramatic changes in orientation of the coninental slope.

The steppy structure of the Brazil Current front (Figure 2), frontal density (Figure 3a) and MKE/EKE ratio (Figure 3d) is striking. It reveals, as expected, that the sinuous topography of the continental slope steers the Brazil Current in the SBB and highlights that the local eddy variability in the region is intimately linked to topography.

### *3.2. Fraction of EKE Accounted for by Compact Eddies*

The eddy kinetic energy map in Figure 3c shows that the SBB, especially the continental slope, is eddy active, with localized hotspots of eddy kinetic energy near inflections of topography. The EKE in Figure 3c is associated with all sea-level variability about MDT. It accounts for small-amplitude (open-contour) meanders of the Brazil Current, large-scale Rossby waves, compact (closed-contour) eddies, etc.

Figure 4a shows a map of the eddy kinetic energy of compact eddies ($EKE_c$); for technical details, see Section 2.4. For a direct comparison with the map of EKE in Figure 3c, we use the same colormap and colorbar limits in both figures. As expected, the $EKE_c$ map shows that the whole oceanic region of the South Brazil Bight hosts energetic compact mesoscale eddies. The map of $EKE_c$ has a similar pattern to the EKE map, with an intensification of the kinetic energy over the continental slope. The fraction of the total eddy kinetic energy accounted for by compact eddies ($EKE_c$/EKE) varies from 30% away from the boundary to about 50% in localized places over the continental slope, with some regions where that contribution is less than 10–20%. The $EKE_c$/EKE fraction in the SBB is roughly consistent with global estimates for the contribution of compact eddies to the total EKE by Chelton et al. [4] and more recently by Martínez-Moreno et al. [37].

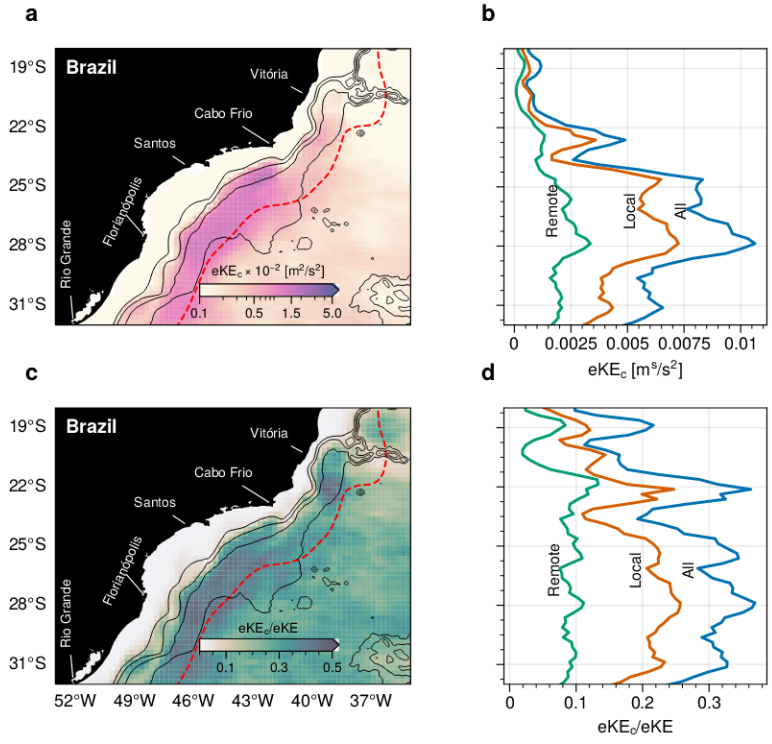


**Figure 4.** (**a**) Kinetic energy due to compact, closed-conttour eddies ($EKE_c$) and (**c**) its ratio to the total eddy kinetic energy. (**b**) The zonal average of $EKE_c$ (blue line) within the Brazil Current domain, defined as the region west of the dashed red curve, and its breakdown into local (orange) and (green) remote eddies. (**d**) Similar to (**b**) but for the energy fraction ($EKE_c$/EKE). Solid black lines in (**a**,**c**) depict the 200, 1000, 2000 and 3000-m isobaths.

#### Breakdown of $EKE_c$ into Local and Remote Eddies

The Eddy Atlas allows us to quantify how much of the compact-eddy variability observed in the Brazil Current region was generated locally versus how much of it was

generated remotely and then propagated into the region. For simplicity, we define the Brazil Current region in the SBB as the area within 200 km of the Brazil Current front MDT front (c.f., Figures 2a and 3a), where the vertical and horizontal shear of the mean Brazil Current jet are concentrated. These mean shears contain copious amounts of energy that are converted to eddies via baroclinic and barotropic instabilities (e.g., [23,38]). (Varying this line by one Rossby radius, around $\pm$30 km, in the east-west direction leads to insignificant quantitative changes in the results.) The red dashed lines in Figure 4a,c mark the outer edge of the Brazil Current region. If an eddy was first observed west of this line, we term it a 'local eddy'. Local eddies are likely generated by instabilities of the Brazil Current and its interaction with the continental slope. If an eddy is first detected east of this line, we term it a 'remote eddy'. Remote eddies can be generated inside or outside our regional box loosely termed SBB. In fact, some of the remote eddies are generated across the South Atlantic, and a few anticyclones may tracked back to the Agulhas Retroflection region [25,26].

Figure 4b,d show the zonally averaged $\mathrm{EKE}_c$ and $\mathrm{EKE}_c/\mathrm{EKE}$ of all compact eddies observed within the Brazil Current domain, and its partition into locally and remotely generated eddies. In other words, the averaged $\mathrm{EKE}_c$ west of the red dashed line is broken down into contributions from eddies generated west (local eddies) and east (remote eddies) of the Brazil Current region outer edge. The zonal average is computed from the 200-m isobath to the outer edge of the Brazil Current region. $\mathrm{EKE}_c$ increases sharply south of 22°S, with localized peaks at 23°S, 24.5°S and 28°S. Over 70% of this $\mathrm{EKE}_c$ in the Brazil Current region is due to compact mesoscale eddies generated locally. On average, local eddies account for 22% of the total EKE observed in the Brazil Current region, and remote eddies account for 8%, with significant spatial variability. The remaining 70% is accounted for by non-compact eddy variability.

Figure 5 show maps of the ratio $\mathrm{EKE}_c/\mathrm{EKE}$ for local and remote eddies and its breakdown by eddy polarity (cyclonic versus anticyclonic). Kinetic energy associated with cyclonic local eddies is highly non-homogeneous, being largely concentrated downstream of significant inflections of the upper continental slope and centered at the 1000-m isobath. Most of these regions are associated with large eddy variability and low MKE/EKE ratios (c.f., Figure 3d). Two regions stand out: the expanses between Cabo Frio and Santos and between Florianópolis and Rio Grande. While the first is a well known hotspot of Brazil Current meander formation through baroclinic conversions (e.g., [24]), the latter is much less studied. Figure 5b suggests that local cyclonic eddies propagate a little downstream, leaving a trace of $\mathrm{EKE}_c$ that decays rapidly from the sharp slope inflections.

Local anticyclones are distributed more broadly over the lower continental slope and continental elevation, centered between the 2000-m and 3000-m isobaths, with an intensification downstream of Santos (Figure 5c). $\mathrm{EKE}_c$ of local eddies decays rapidly east of the red dashed line in Figure 5a–c. In other words, while local eddies may propagate over the continental slope, there is very little leakage of $\mathrm{EKE}_c$ from the Brazil Current region towards east.

The kinetic energy of remote eddies is distributed fairly homogeneously to the east of the Brazil Current region outer edge (Figure 5d). The partition into cyclonic and anticyclonic $\mathrm{EKE}_c$ is patchier. One interesting feature is the concentration of cyclonic $\mathrm{EKE}_c$ at the edges of the São Paulo Plateau (Figure 5e). Figure 5d–f further show spatial details of the small but significant leakage of remote $\mathrm{EKE}_c$ into the Brazil Current region. The ratio $\mathrm{EKE}_c/\mathrm{EKE}$ of remote eddies in the Brazil Current region is less than 0.1. Interestingly, remote anticyclones seem to propagate farther upslope than remote cyclones. Anticyclonic remote $\mathrm{EKE}_c$ is especially large south of Vitória. The relevance of remote signals in region has previously been reported by Napolitano et al. [28], who used a regional numerical model to show that remote closed-contour anticyclones exchange energy with the western boundary currents at 18°S–20°S. The São Paulo Plateau also hosts significant anticyclonic $\mathrm{EKE}_c$, and remote anticyclones seem to make to the upper slope in the region between Santos and Florianópolis. That said, we note that remote anticyclonic $\mathrm{EKE}_c$ is about one

third of the local anticyclonic $EKE_c$, accounting for less than 10% of the total anticyclonic EKE in the Brazil Current region.

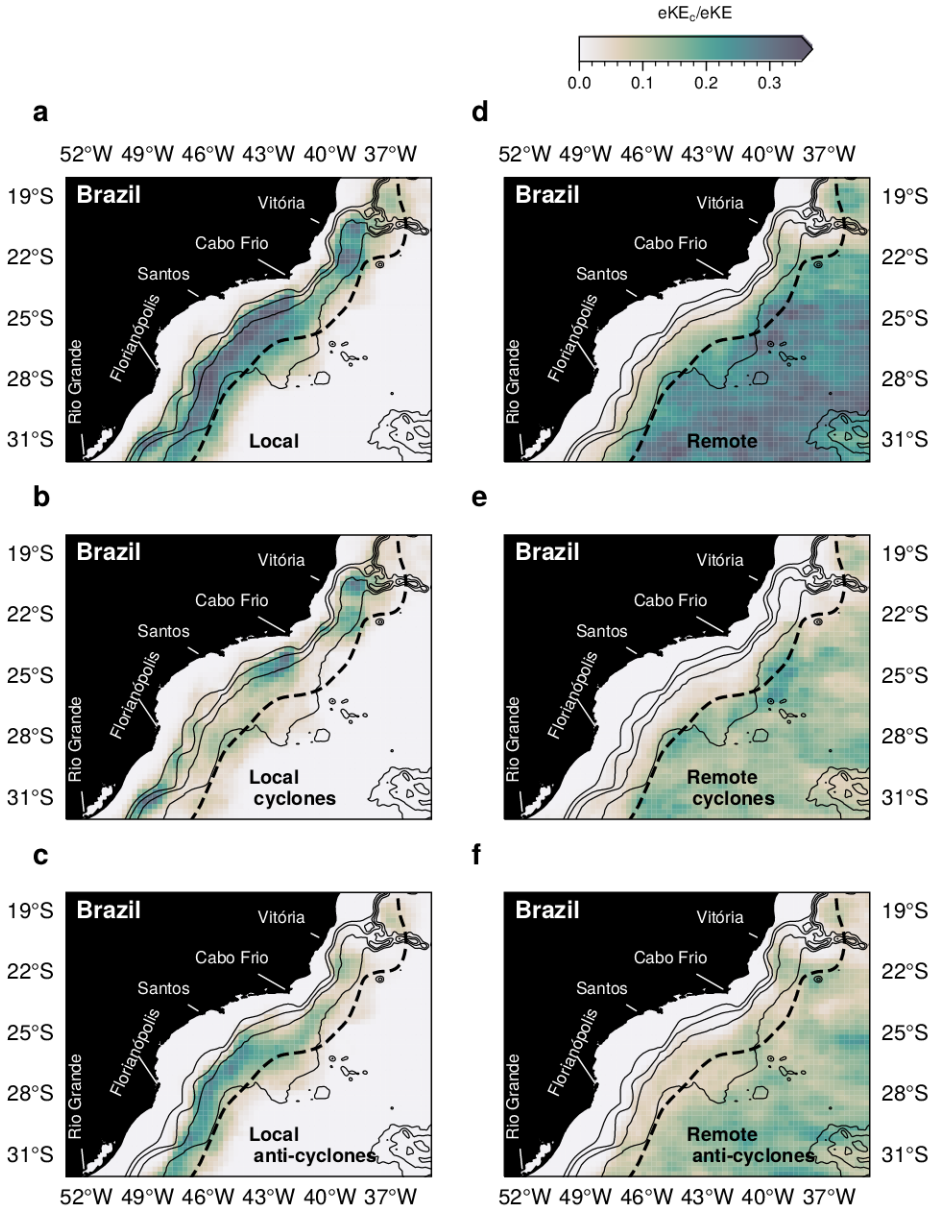


**Figure 5.** (**a**) Fraction of kinetic energy accounted for by compact, closed-contour eddies generated locally in the Brazil Current region, defined as eddies first identified west of the dashed red line, and its breakdown into the kinetic energy of (**b**) cyclones and (**c**) anticyclones. (**d**–**f**) Similar to (**a**–**c**) but for compact, closed-contour eddies generated remotely. The black dashed line marks a distance of 200 km from the Brazil Current front in Figure 4, defining the Brazil Current region. Solid black lines depict the 200, 1000, 2000 and 3000-m isobaths.

### *3.3. Eddy Properties*

The analysis of eddy kinetic energy above quantifies the contribution of compact eddies to the geostrophic variability in the SBB. Compact eddies account for about 20–50% of the total surface eddy kinetic energy observed in the Brazil Current region, with local eddies contributing the most. The analysis also reveals interesting patterns of kinetic energy due to local and remote eddies. To further characterize and explain these patterns, we analyze the statistics of key eddy properties in the META3.2 DT Eddy Atlas. The global distribution and significance of such properties has been discussed based on previous eddy

censuses, beginning with Chelton et al. [3] and Chelton et al. [4]. Several follow-up studies also discussed these properties and their implications for the eddy variability in different regions of the world ocean (e.g., [14,16]). Our focus here is on the differences between eddy properties of local and remote eddies in the SBB, and their implications for the eddy kinetic energy distribution in the Brazil Current region (Figures 4 and 5).

#### 3.3.1. Origin and Propagation

Provided an eddy has not propagated much during over its initial growth—during which its small amplitudes are inaccessible to current satellite altimeters—the location of first detection is a good approximation to the eddy's generation site. Figure 6 shows the distribution of first-detection location of eddies in the SBB. Figure 6a shows eddies that were either generated locally in the Brazil Current region, west of the black dashed line, or eddies that eventually propagated into it. Figure 6b shows eddies generated outside the Brazil Current region (i.e., east of the black dashed line) and that were never detected west of the black dashed line. A few interesting patterns emerge. First, there is a preference for generation of local cyclones in the upper slope, at or downstream of sharp inflections of the isobaths, as anticipated by the EKE analysis. These are the regions from which the trail of cyclonic $EKE_c$ emanates (c.f., Figure 5b). A prominent cyclonic eddy generation site is the upper-slope region off Cabo Frio, consistent with previous studies (e.g., [24,39]). Two other cyclonic eddy formation hotspots are apparent in Figure 6a (see concentration of blue dots south of Florianópolis). While local cyclones are generated almost exclusively near inflections of the upper continental slope, the origin of anticyclones occurs by and large on the lower slope, between the 2000-m and 3000-m isobaths, and is far more uniformly distributed across the SBB.

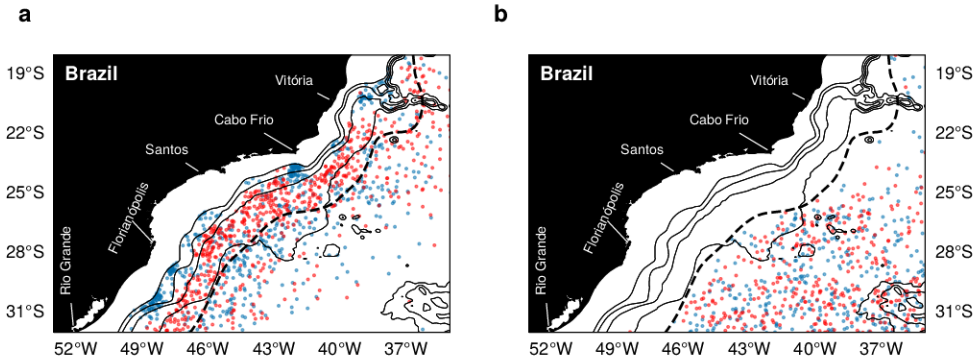


**Figure 6.** Location of first detection of unique long-lived compact eddies in the South Brazil Bight, with blue dots representing cyclones and red dots anticyclones. (**a**) Local Brazil Current eddies and remote eddies that at some time were observed in the Brazil Current region, west of the of black dashed line. (**b**) Remote eddies that were never observed west of the black dashed line. Several remote eddies have origins east of 35°W and thus are not represented in (**b**). Solid black lines depict the 200, 1000, 2000 and 3000-m isobaths.

Most remote eddies, both cyclonic and anticyclonic, that eventually propagated into the Brazil Current region were generated not farther than 300 km off the 3000-m isobath, with nearly uniform distribution in latitude; a few eddies were generated east of 35°W (not shown). In contrast, remote eddies that were never detected in the Brazil Current region have origin locations concentrated south of 25°S and uniformly distributed in longitude. A large number of remote eddies that were detected in the SBB, but never in the Brazil Current region, were generated hundreds of kilometers east of 35°W (not shown), and some were generated all the way across the South Atlantic (c.f., [29]).

As a first look into eddy propagation, Figure 7a shows trajectories of 20 randomly selected eddies that were either generated in or propagated into the Brazil Current region, and Figure 7b shows the trajectories of 20 randomly selected eddies that were never detected in the Brazil Current region. (We tested the random selection with several different random

seeds to ensure that these trajectories are representative of all eddies, and we recorded the final seed for replicability.) Local eddies largely propagate due southwest, in the direction of the Brazil Current. As expected, remote eddies propagate due west; however, those remote eddies that eventually move into the Brazil Current region, west of the black dashed line, veer southwestward, suggesting an interaction with the background Brazil Current flow. There are exceptions to these general propagation patterns. For example, the anticyclone generated near the edge of the Brazil Current region at 22°S initially propagates due west/southwest and then veers northward. Further, one remote cyclone generated over a seamount at 26°S moves northwards. Most of the eddies propagate about 100–300 km from first to last detection. One clear exception is a remotely generated anticyclone that propagated into the Brazil Current region. This eddy was generated far east of 35°W and propagated over 1000 km over its lifetime.

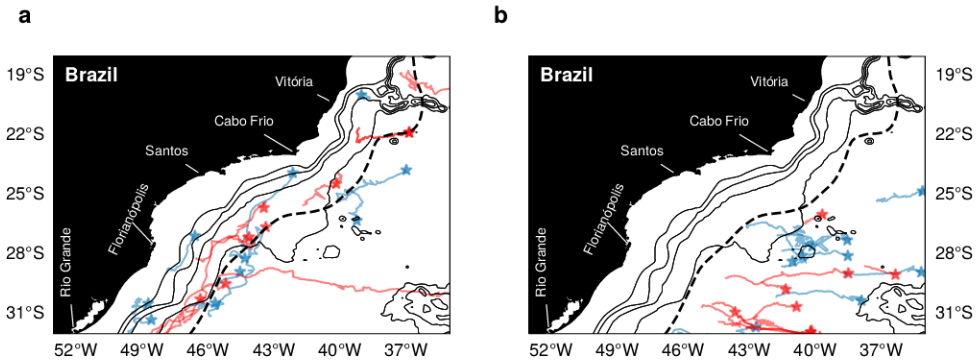


**Figure 7.** Randomly selected example trajectories of unique long-lived compact eddies in the South Brazil Bight, with blue lines representing cyclones and red lines anticyclones. (**a**) Local Brazil Current eddies and remote eddies that at some time were observed in the Brazil Current region, west of the of black dashed line. Stars represent the location of first detection of the eddy (cf., Figure 6) (**b**) Remote eddies that were never observed west of the black dashed line. The origin of one anti-cyclone in (**a**) is not shown because this eddy was generated west of 35°W, outside the regional box. Solid black lines depict the 200, 1000, 2000 and 3000-m isobaths.

To characterize eddy propagation statistically, we show in Figure 8 the probability density and cumulative density functions of total displacement of the eddies, from first to last detection. On average, local anticyclones propagate slightly farther (259 ± 11 km) than local cyclones (228 ± 10 km), but the overall distribution and eddy counts are similar for both rotations (see Figure 8a,d). About 25% of local eddies propagate less than 100 km and 75% propagate less than 250 km. In contrast, remote eddies that were eventually detected in the Brazil Current region have propagated longer distances, with anticyclones propagating, on average, 40% farther than cyclones, 560 ± 17 km vs. 325 ± 14 km, respectively. A few anticyclones have propagated more than 5000 km (see inset in Figure 8b). These are Agulhas Rings whose remnants eventually arrive at the Brazil Current region [25,26]. However, the vast majority of the remote eddies that were eventually detected in the Brazil Current region were generated west of the Mid-Atlantic Ridge; for example, 75% of the anticyclones (cyclones) propagated less than 510 km (350 km).

Several hundred remote eddies propagated into the South Brazil Bight but not into the Brazil Current region. Of those, 29 anticyclones originated across the South Atlantic, traveling over 4000 km; however, the vast majority of the remote eddies have traveled a much shorter distances, with 75% propagating less than 400 km. One interesting property of remote eddies is that the asymmetry between cyclones and anticyclones is much more pronounced in the eddies that eventually propagated into the Brazil Current region (compare Figure 8e,f).

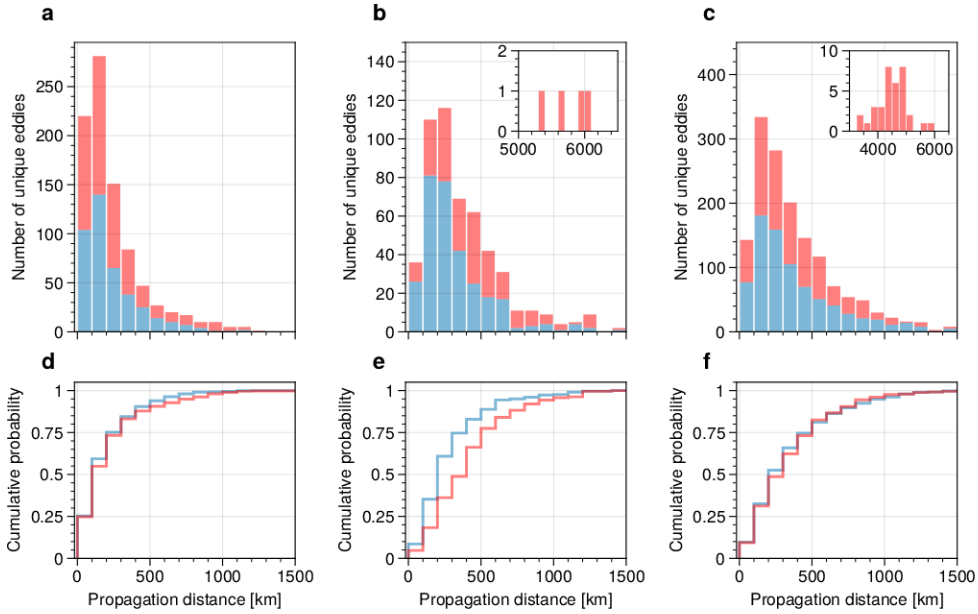


**Figure 8.** Statistics of total propagation distance of unique compact eddies that were at some point in their lifespan observed in the regional box that loosely defines the South Brazil Bight. The upper panels (**a**–**c**) are histograms of propagation distance, with blue bars representing cyclones and red bars anticyclones. These are stacked histograms, so the number of anticyclones in each bins is the difference between its top and base. The lower panels (**d**–**f**) are cumulative histograms associated with (**a**–**c**). Left panels (**a**,**d**) are histograms for local eddies, middle panels (**b**,**e**) for remote eddies that eventually propagated into the Brazil Current region, west of the black dashed line in Figure 7, and right panels (**c**,**f**) are remote eddies that at some point in their lifespan were observed in the regional box but never moved into the Brazil Current region. The insets in (**b**,**c**) show a few remote anticyclones that were generated near the Agulhas Retroflection region and tracked across the South Atlantic.

Figure 9 shows polar scatter plots of propagation speeds colored by the nonlinear parameter, defined as the ratio between swirl and propagation speeds $u_\theta/c_p$ [3,4]. Eddies that have relatively large amplitudes and slow propagation speed are more nonlinear. The largest the nonlinear parameter, the highest the likelihood of an eddy trapping fluid within it. As discussed in the literature, most compact mesoscale eddies in the global ocean are nonlinear by this metric, suggesting those eddies may transport fluid properties for long distances [4]. In the SBB, virtually all eddies satisfy $u_\theta/c_p > 1$. Figure 9a,b shows that most local eddies are strongly nonlinear and, as illustrated in Figure 7, propagate due southwest. Their propagation speeds vary from 1 to 10 km/day, with a large number of cyclones and anticyclones moving slower than 2 km/day. The remote eddies largely propagate due west. Interestingly, of the remote eddies that were eventually detected in the Brazil Current regions, cyclones are more nonlinear than anticyclones: there are less anticyclones that propagate at slower speeds, and this is consistent with the longer travel distances of remote anticyclones (c.f., Figure 8d). The differences between cyclones and anticyclones are less obvious for the eddies that were never detected in the Brazil Current region.

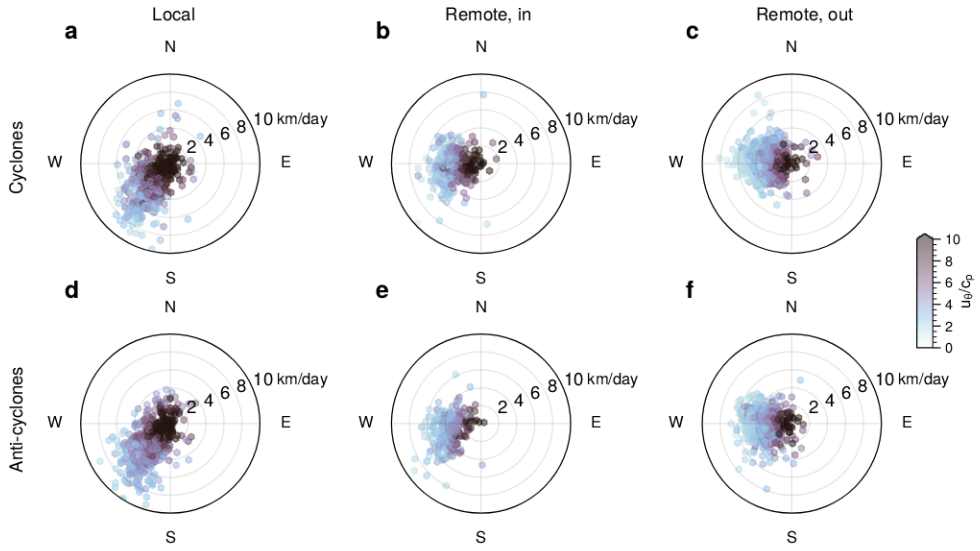


**Figure 9.** Scatter plots of eddy propagation speed colored by the nonlinear parameter ($u_\theta/c_p$) of unique compact eddies in the South Brazil Bight. Upper panels (**a**–**c**) show cyclones and lower panels (**d**–**f**) anticyclones. As in Figure 8, the left panels (**a**,**d**) show local Brazil Current eddies, generated west of the black dashed line in Figure 7, the middle panels (**b**,**e**) show remote eddies that eventually propagated into the Brazil Current region, and the right panels (**c**,**f**) remote eddies that were never observed west of the black dashed line in Figure 7.

#### 3.3.2. Amplitude, Radius, Lifetime, and Speed

Table 1 summarizes the averaged eddy properties for local and remote eddies in the SBB. Amplitude (Amp.), effective radius (Ef. rad.), speed radius (Sp. rad.) and average speed (Avg. sp.) are averaged over the lifetime (L. time) of each eddy (the number of days elapsed between first and last detection); see Section 2.1 and Pegliasco et al. [30] for a detailed definition of these properties. The means in Table 1 are averages over unique eddies detected over the altimetric record (1993–2021), with uncertainties representing one standard error (each unique eddy contributes one degree of freedom). The number of unique eddies for each category of rotation and generation/propagation is so large that the standard errors are fractional. In general, statistically significant differences in eddy properties exist across categories. For local eddies, there is a slight preference for anticyclones over cyclones (794 vs. 734). The opposite is true for remote eddies. For remote eddies that were never detected within the Brazil Current region, the preference for cyclones is slight (930 vs. 868), but for remote eddies that propagated into the Brazil Current region, this preference is more significant (340 vs. 235).

The mean amplitude of the eddies is similar across categories (around 5 cm), except for remote eddies that never propagated into the Brazil Current region, whose cyclones have have significantly smaller amplitudes ($4.1 \pm 0.1$ cm) than anticyclones ($4.7 \pm 0.1$ cm). Local eddies have a lifespan of about 47 days, with no statistically significant differences between cyclones and anticyclones. Remote anticyclones, however, are significantly more long-lived than remote cyclones, with a difference in lifetime of about 40 days.

In general, anticyclones are bigger than cyclones by about 10 km, with the exception of remote eddies that never propagated into the Brazil Current region, which have smaller differences in size between rotation categories. The radius associated with the contour of maximum swirl speed (speed radius) is consistently 7–10 km smaller than the radius associated with the outermost closed contour (effective radius). Finally, local eddies have average speeds slightly bigger than remote eddies (about 22 vs. 18 cm/s).

**Table 1.** Mean and standard error of key properties of compact, closed-contour cyclonic (cyc) and anticyclonic (acy) mesoscale eddies in the South Brazil Bight. The numbers in parenthesis represent the total number of unique eddies identified over the altimetric record (1993–2021), and the statistics are based on averaged properties over each eddy's lifetime; the statistics only counts eddies with time-averaged amplitude greater than 2.5 cm, significantly above the altimeter noise. Local eddies were first observed within the Brazil Current domain, west of the dashed line in Figure 6, while remote eddies were first detected outside the Brazil Current region, east of the the dashed line. Remote-in eddies were eventually detected west of the dashed line; remote-out eddies were never detected west of that line. See Section 2.1 for a description of the eddy properties in the META3.2 DT Eddy Atlas.

| | **Local** | | **Remote, in** | | **Remote, out** | |
|---|---|---|---|---|---|---|
| | cyc (732) | acy (794) | cyc (340) | acy (235) | cyc (930) | acy (868) |
| Amplitude [cm] | $4.8 \pm 0.1$ | $4.9 \pm 0.1$ | $5.1 \pm 0.0$ | $5.3 \pm 0.2$ | $4.1 \pm 0.1$ | $4.7 \pm 0.1$ |
| Life time [day] | $46 \pm 2$ | $48 \pm 2$ | $92 \pm 5$ | $134 \pm 9$ | $103 \pm 3$ | $145 \pm 5$ |
| Effec. radius [km] | $57 \pm 0$ | $67 \pm 1$ | $70 \pm 1$ | $80 \pm 2$ | $77 \pm 1$ | $81 \pm 1$ |
| Speed rad. [km] | $48 \pm 0$ | $60 \pm 1$ | $58 \pm 1$ | $68 \pm 1$ | $65 \pm 1$ | $68 \pm 1$ |
| Avg. speed [cm/s] | $22.2 \pm 0.2$ | $21.6 \pm 0.2$ | $18.1 \pm 0.2$ | $18.1 \pm 0.3$ | $13.6 \pm 0.1$ | $14.3 \pm 0.1$ |

## 4. Conclusions

The South Brazil Bight (SBB) has long been known to be a secondary maximum of eddy kinetic energy in the Southwestern Atlantic, and there is growing evidence that the region hosts strong westward-propagating remote eddies. Some of these might be generated all across the South Atlantic and might even reach and interact with the Brazil Current [25–29]. Taking advantage of a new Eddy Atlas that contains sea-level contours for each eddy observation, this study aimed at quantifying how much of the mesoscale variability in the Brazil Current region is accounted for by compact, closed-contour eddies, separating that variability into eddies generated locally from those generated remotely.

To that end, we first characterized the position of the Brazil Current sea-level front and its variability. The front is well-defined and occupies the SBB upper continental slope most of the time, with the exception of regions downstream of sharp inflections of the isobaths, where the front position displays large variability (Figure 3a). These regions are eddy hotspots, where the eddy kinetic energy (EKE) far exceeds the mean kinetic energy (MKE).

Overall, compact, closed-contour eddies account for 30–50% of the surface geostrophic EKE in the SBB, with an enhancement in the Brazil Current region—defined as the area within 200 km of the mean Brazil Current front. The remaining 50% is likely accounted for by other types of eddy variability, such as small amplitude meanders (with undetectable closed contours) and Rosbby waves (e.g., [8,40]). Virtually all compact eddies in the SBB are nonlinear by the metric of swirl speeds exceeding the propagation speeds, and most of them are strongly nonlinear. Eddies generated locally in the Brazil Current region—likely by instabilities of the current and its interaction with topography—are in general more nonlinear than eddies generated remotely. In contrast to remote eddies, which (as most eddies in the global ocean) propagate due west (e.g., [4]), local eddies largely propagate due southwest, in the direction of the Brazil Current. Most remote eddies that eventually arrive in the Brazil Current region tend to veer southwestward, except for a few eddies in the northern part of the domain that tend to do the opposite, possibly under the influence of the Intermediate Western Boundary Current (e.g., [28]).

Hence, there are significant differences between the averaged properties of local and remote eddies summarized in Table 1, showing that—on average—remote eddies are bigger but weaker than local eddies. While statistically robust, the averaged properties in Table 1 should be interpreted with caution. Most eddy properties have wide-range, skewed and long-tailed distributions. As an example, Figure 10 shows violin plots for a few properties of local eddies. Although the average amplitude of local anticyclones is about 5 cm, many have amplitudes larger than 15 cm. Similarly, local cyclones have an averaged lifetime of $46 \pm 2$ days, but a number of cyclones lived longer than 200 days, and some lived longer

than 1 year. The distributions of properties of remote eddies, especially remote anticyclones, are even more long-tailed (not shown).

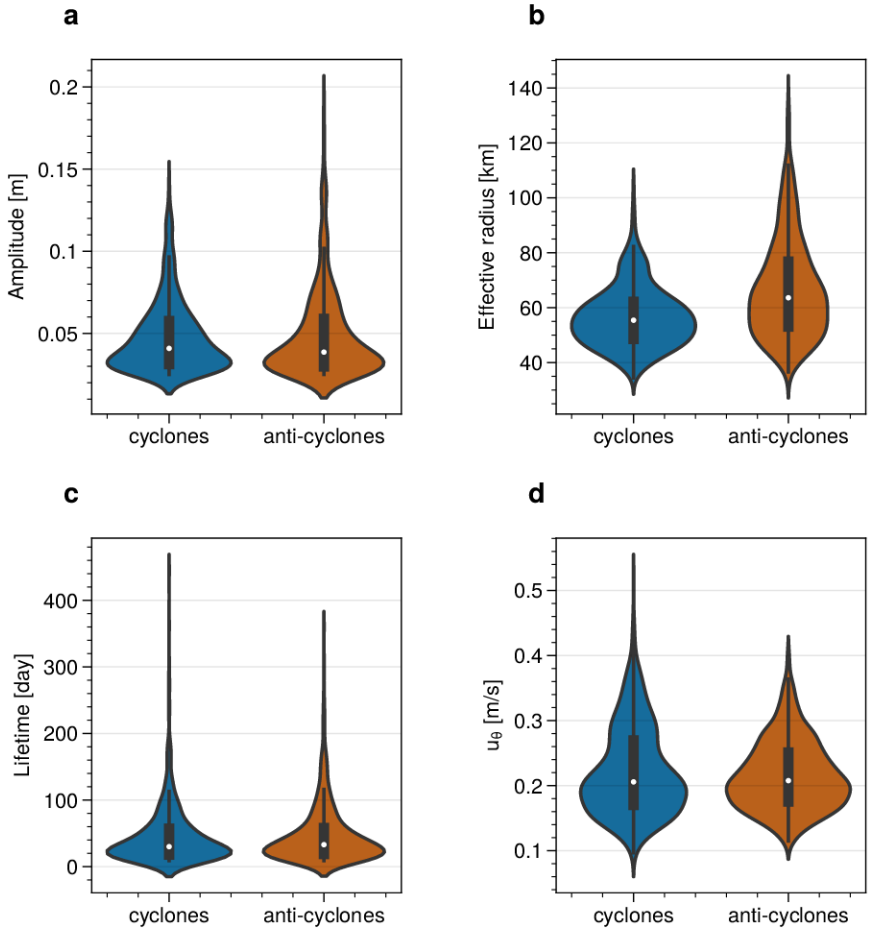


**Figure 10.** A visualization of the statistics of (**a**) amplitude, (**b**) effective radius, (**c**) lifetime and (**d**) average speed for local eddies in the South Brazil Bight. These violin plots show the extreme values, median (white circle), first and third quartiles (black rectangle), and the distributions of the data. Mean and standard error statistics for these, as well as for remote eddies, are shown in Table 1.

Following the work by Chelton et al. [3] and subsequent regional studies (e.g., [14–17]), there have been a number of studies that point out limitations with tracking of mesoscale eddies based on the identification of closed contours in high-pass filtered snapshots of sea level. One major criticism to this Eulerian eddy tracking is that sea-level contours are not material lines and thus the eddies identified by this method may not be coherent Lagrangian structures (e.g., [31,41,42]). This implies that the sea-level eddies discussed in this study may not trap and transport water for long distances, despite having swirl speeds much larger than propagation speeds, and their role in material transport may be overstated. For example, using an estimation of coherence based on dynamical systems, Wang et al. [41] concludes that material transport by Agulhas Rings in the South Atlantic is less than previously reported. Another criticism specific to the algorithms in Chelton et al. [4] and in META3.2 DT is that they do not allow for splitting of merging of eddies. Including splitting and merging of eddies may increase the number of remote eddies that arrive in the SBB [26,29]; however, splitting and merging likely increase mixing of eddies with the surrounding waters. Thus the eddies in Ioannou et al. [29] that went through multiple splittings and mergings are even less likely to transport material into the SBB than the unique remote eddies in META3.2 DT.

Despite the caveats outlined above, there are several results from our analysis that are robust and provide a benchmark for future observational and numerical studies in the region. First, mesoscale compact eddies account for 30–50% of the eddy kinetic energy in the SBB. Further, local Brazil Current eddies account for most of the compact mesoscale eddy variability observed in the Brazil Current region; remote eddies account for only a small fraction of the compact mesoscale eddy variability (less than 25% of the compact eddy kinetic energy, which is less than 10% of the total eddy kinetic energy). Second, compact eddies that were generated across the South Atlantic, such as remnant Agulhas Rings (e.g., [25,26]), contribute an insignificant fraction of eddy kinetic energy to the total mesoscale variability in the Brazil Current region. It is possible, of course, that these decaying remote eddies, while moving through a field with varying background potential vorticity, generate non-compact eddy variability that propagate into the SBB, which in turn may affect the meandering and low-frequency variability of the Brazil Current [40]. Investigating the interplay between compact and non-compact eddy variability in the SBB is left for a future study.

In closing, we note that this study points to a close relationship between local cyclonic compact eddy variability and topography, especially sharp inflections of the upper continental slope. While not unexpected, the relationship is striking and our results highlight three local hotspots of Brazil Current cyclonic eddy generation, two of which are poorly studied. Theoretical and numerical models that ignore or over-idealized the local bathymetry (e.g., [23,24]) are unlikely to capture the Brazil Current cyclogenesis correctly. A model hierarchy is called for.

**Author Contributions:** Conceptualization, C.B.R. and I.T.S.-S.; methodology, C.B.R. and I.T.S.-S.; software, I.T.S.-S. and C.B.R.; validation, I.T.S.-S. and C.B.R.; formal analysis, C.B.R. and I.T.S.-S.; investigation, I.T.S.-S. and C.B.R.; resources, C.B.R.; writing—original draft preparation, C.B.R.; writing—review and editing, C.B.R. and I.T.S.-S. All authors have read and agreed to the published version of the manuscript.

**Funding:** This research was funded by the National Science Foundation award number 2146729.

**Data Availability Statement:** All data used in this study are available online in two different platforms. The gridded sea-level anomalies product can be obtained at Copernicus Marine Service (https://marine.copernicus.eu, accessed on 5 April 2022). The mean dynamic topography (MDT-CNES-CLS18) and the META3.2 DT can be obtained from Aviso+ (https://www.aviso.altimetry.fr/en/data/products/auxiliary-products/mdt/mdt-global-cnes-cls18.html (accessed on 5 April 2022) and https://www.aviso.altimetry.fr/en/data/products/value-added-products/global-mesoscale-eddy-trajectory-product/meta3-2-dt.html, accessed on 5 April 2022). For reference, the identification number of each product is provided in Section 2.1.

**Acknowledgments:** The authors had useful discussions with Ilson Silveira and his graduate students at IO-USP, Brazil.

**Conflicts of Interest:** The authors declare no conflict of interest.

## References

1. Chelton, D.B.; Ries, J.C.; Haines, B.J.; Fu, L.L.; Callahan, P.S. Satellite altimetry. In *International Geophysics*; Elsevier: Amsterdam, The Netherlands, 2001; Volume 69, pp. 1–131.
2. Ferrari, R.; Wunsch, C. Ocean circulation kinetic energy: Reservoirs, sources, and sinks. *Annu. Rev. Fluid Mech.* **2009**, *41*, 253–282. [CrossRef]
3. Chelton, D.B.; Schlax, M.G.; Samelson, R.M.; de Szoeke, R.A. Global observations of large oceanic eddies. *Geophys. Res. Lett.* **2007**, *34*, L15606. [CrossRef]
4. Chelton, D.B.; Schlax, M.G.; Samelson, R.M. Global observations of nonlinear mesoscale eddies. *Prog. Oceanogr.* **2011**, *91*, 167–216. [CrossRef]
5. Chelton, D.B.; Schlax, M.G. Global observations of oceanic Rossby waves. *Science* **1996**, *272*, 234–238. [CrossRef]
6. Polito, P.S.; Cornillon, P. Long baroclinic Rossby waves detected by TOPEX/POSEIDON. *J. Geophys. Res. Ocean.* **1997**, *102*, 3215–3235. [CrossRef]
7. Oliveira, F.; Polito, P.S. Characterization of westward propagating signals in the South Atlantic from altimeter and radiometer records. *Remote Sens. Environ.* **2013**, *134*, 367–376. [CrossRef]

8. Polito, P.S.; Sato, O.T. Do eddies ride on Rossby waves? *J. Geophys. Res. Ocean.* **2015**, *120*, 5417–5435. [CrossRef]
9. Mode-Group. The mid-ocean dynamics experiment. *Deep Sea Res.* **1978**, *25*, 859–910. [CrossRef]
10. Gill, A.; Green, J.; Simmons, A. Energy partition in the large-scale ocean circulation and the production of mid-ocean eddies. *Deep Sea Res. Oceanogr. Abstr.* **1974**, *21*, 499–528. [CrossRef]
11. Abernathey, R.; Marshall, J. Global surface eddy diffusivities derived from satellite altimetry. *J. Geophys. Res. Ocean.* **2013**, *118*, 901–916. [CrossRef]
12. Gaube, P.; McGillicuddy, D.J., Jr.; Chelton, D.B.; Behrenfeld, M.J.; Strutton, P.G. Regional variations in the influence of mesoscale eddies on near-surface chlorophyll. *J. Geophys. Res. Ocean.* **2014**, *119*, 8195–8220. [CrossRef]
13. Groeskamp, S.; LaCasce, J.H.; McDougall, T.J.; Rogé, M. Full-Depth Global Estimates of Ocean Mesoscale Eddy Mixing from Observations and Theory. *Geophys. Res. Lett.* **2020**, *47*, e2020GL089425. [CrossRef]
14. Chaigneau, A.; Gizolme, A.; Grados, C. Mesoscale eddies off Peru in altimeter records: Identification algorithms and eddy spatio-temporal patterns. *Prog. Oceanogr.* **2008**, *79*, 106–119. [CrossRef]
15. Chaigneau, A.; Le Texier, M.; Eldin, G.; Grados, C.; Pizarro, O. Vertical structure of mesoscale eddies in the eastern South Pacific Ocean: A composite analysis from altimetry and Argo profiling floats. *J. Geophys. Res. Ocean.* **2011**, *116*. [CrossRef]
16. Castelao, R.M.; He, R. Mesoscale eddies in the South Atlantic bight. *J. Geophys. Res. Ocean.* **2013**, *118*, 5720–5731. [CrossRef]
17. Pegliasco, C.; Chaigneau, A.; Morrow, R. Main eddy vertical structures observed in the four major Eastern Boundary Upwelling Systems. *J. Geophys. Res. Ocean.* **2015**, *120*, 6008–6033. [CrossRef]
18. Aguedjou, H.; Dadou, I.; Chaigneau, A.; Morel, Y.; Alory, G. Eddies in the Tropical Atlantic Ocean and their seasonal variability. *Geophys. Res. Lett.* **2019**, *46*, 12156–12164. [CrossRef]
19. De Ruijter, W.; Biastoch, A.; Drijfhout, S.; Lutjeharms, J.; Matano, R.; Pichevin, T.; Van Leeuwen, P.; Weijer, W. Indian-Atlantic interocean exchange: Dynamics, estimation and impact. *J. Geophys. Res. Ocean.* **1999**, *104*, 20885–20910. [CrossRef]
20. Beal, L.M.; De Ruijter, W.P.; Biastoch, A.; Zahn, R. On the role of the Agulhas system in ocean circulation and climate. *Nature* **2011**, *472*, 429–436. [CrossRef]
21. Gordon, A.L. Brazil-Malvinas Confluence–1984. *Deep Sea Res. Part A Oceanogr. Res. Pap.* **1989**, *36*, 359–384. [CrossRef]
22. Goni, G.; Kamholz, S.; Garzoli, S.; Olson, D. Dynamics of the Brazil-Malvinas Confluence based on inverted echo sounders and altimetry. *J. Geophys. Res. Ocean.* **1996**, *101*, 16273–16289. [CrossRef]
23. Silveira, I.; Lima, J.; Schmidt, A.; Ceccopieri, W.; Sartori, A.; Franscisco, C.; Fontes, R. Is the meander growth in the Brazil Current system off Southeast Brazil due to baroclinic instability? *Dyn. Atmos. Ocean.* **2008**, *45*, 187–207. [CrossRef]
24. Rocha, C.B.; Silveira, I.C.; Castro, B.M.; Lima, J.A.M. Vertical structure, energetics, and dynamics of the Brazil Current System at 22°S–28°S. *J. Geophys. Res. Ocean.* **2014**, *119*, 52–69. doi: 10.1002/2013JC009143. [CrossRef]
25. Guerra, L.A.A.; Paiva, A.M.; Chassignet, E.P. On the translation of Agulhas rings to the western South Atlantic Ocean. *Deep Sea Res. Part I Oceanogr. Res. Pap.* **2018**, *139*, 104–113. [CrossRef]
26. Laxenaire, R.; Speich, S.; Blanke, B.; Chaigneau, A.; Pegliasco, C.; Stegner, A. Anticyclonic eddies connecting the western boundaries of Indian and Atlantic oceans. *J. Geophys. Res. Ocean.* **2018**, *123*, 7651–7677. [CrossRef]
27. Laxenaire, R.; Speich, S.; Stegner, A. Evolution of the Thermohaline Structure of One Agulhas Ring Reconstructed from Satellite Altimetry and Argo Floats. *J. Geophys. Res. Ocean.* **2019**, *124*, 8969–9003. [CrossRef]
28. Napolitano, D.C.; Silveira, I.C.; Rocha, C.B.; Flierl, G.R.; Calil, P.H.; Martins, R.P. On the Steadiness and Instability of the Intermediate Western Boundary Current between 24 and 18S. *J. Phys. Oceanogr.* **2019**, *49*, 3127–3143. [CrossRef]
29. Ioannou, A.; Speich, S.; Laxenaire, R. Characterizing mesoscale eddies of eastern upwelling origins in the Atlantic Ocean and their role in offshore transport. *Front. Mar. Sci.* **2022**, *9*, 835260. [CrossRef]
30. Pegliasco, C.; Delepoulle, A.; Mason, E.; Morrow, R.; Faugère, Y.; Dibarboure, G. META3.1exp: A new global mesoscale eddy trajectory atlas derived from altimetry. *Earth Syst. Sci. Data* **2022**, *14*, 1087–1107. [CrossRef]
31. Abernathey, R.; Haller, G. Transport by lagrangian vortices in the Eastern Pacific. *J. Phys. Oceanogr.* **2018**, *48*, 667–685. [CrossRef]
32. Mulet, S.; Rio, M.H.; Etienne, H.; Artana, C.; Cancet, M.; Dibarboure, G.; Feng, H.; Husson, R.; Picot, N.; Provost, C.; et al. The new CNES-CLS18 global mean dynamic topography. *Ocean Sci.* **2021**, *17*, 789–808. [CrossRef]
33. Mason, E.; Pascual, A.; McWilliams, J.C. A new sea surface height–based code for oceanic mesoscale eddy tracking. *J. Atmos. Ocean. Technol.* **2014**, *31*, 1181–1188. [CrossRef]
34. Drouin, K.L.; Lozier, M.S.; Johns, W.E. Variability and trends of the South Atlantic subtropical gyre. *J. Geophys. Res. Ocean.* **2021**, *126*, e2020JC016405. [CrossRef]
35. Lorenzzetti, J.A.; Stech, J.L.; Mello Filho, W.L.; Assireu, A.T. Satellite observation of Brazil Current inshore thermal front in the SW South Atlantic: Space/time variability and sea surface temperatures. *Cont. Shelf Res.* **2009**, *29*, 2061–2068. [CrossRef]
36. Garfield, N., III. The Brazil Current at Subtropical Latitudes. Ph.D. Thesis, University of Rhode Island, Narragansett, RI, USA, 1990.
37. Martínez-Moreno, J.; McC. Hogg, A.; England, M.H. Climatology, seasonality, and trends of spatially coherent ocean eddies. *J. Geophys. Res. Ocean.* **2022**, *127*, e2021JC017453. [CrossRef]
38. Oliveira, L.R.; Piola, A.R.; Mata, M.M.; Soares, I.D. Brazil Current surface circulation and energetics observed from drifting buoys. *J. Geophys. Res. Ocean.* **2009**, *114*, C10006. [CrossRef]
39. Campos, E.J.; Gonçalves, J.; Ikeda, Y. Water mass characteristics and geostrophic circulation in the South Brazil Bight: Summer of 1991. *J. Geophys. Res. Ocean.* **1995**, *100*, 18537–18550. [CrossRef]

40. Majumder, S.; Goes, M.; Polito, P.S.; Lumpkin, R.; Schmid, C.; Lopez, H. Propagating modes of variability and their impact on the western boundary current in the South Atlantic. *J. Geophys. Res. Ocean.* **2019**, *124*, 3168–3185. [CrossRef]
41. Wang, Y.; Olascoaga, M.J.; Beron-Vera, F.J. Coherent water transport across the South Atlantic. *Geophys. Res. Lett.* **2015**, *42*, 4072–4079. [CrossRef]
42. Andrade-Canto, F.; Beron-Vera, F. Do eddies connect the tropical Atlantic Ocean and the Gulf of Mexico? *arXiv* **2022**, arXiv:2205.04835.